THIS PREPRINT APPEARS IN ITS FINAL FORM IN THE JOURNAL OF THE FRANKLIN INSTITUTE, VOL.349, NO.2 (2012), PP.510-530. (DOI:10.1016/J.JFRANKLIN.2011.06.026)

Fault reconstruction using a LPV sliding mode observer for a class of LPV systems

H. Alwi, C. Edwards, and A. Marcos

Abstract

This paper proposes a new sliding mode observer for fault reconstruction, applicable for a class of Linear Parameter Varying (LPV) systems. Observer schemes for actuator and sensor fault reconstruction are presented. For the actuator fault reconstruction scheme, a virtual system comprising the system matrix and a fixed input distribution matrix is used for the design of the observer. The fixed input distribution matrix is instrumental in simplifying the synthesis procedure to create the observer gains to ensure a stable closed-loop reduced order sliding motion. The 'output error injection signals' from the observer are used as the basis for reconstructing the fault signals. For the sensor fault observer design, augmenting the LPV system with a filtered version of the faulty measurements allows the sensor fault reconstruction problem to be posed as an actuator fault reconstruction scenario. Simulation tests based on a high-fidelity nonlinear model of a transport aircraft have been used to demonstrate the proposed actuator and sensor FDI schemes. The simulation results show their efficacy.

I. Introduction

Fault Detection and Isolation (FDI) is a vital component of (active) Fault Tolerant Control (FTC) schemes [1], [2]. The FDI scheme is responsible for providing timely information about the location of any faults/failures within the system being monitored, thus allowing for example, controller reconfiguration. A challenging problem in FDI design, especially for aerospace applications, is dealing with changes in the operating conditions. Such changes must not result in false alarms and unnecessary controller reconfiguration. Although there are nonlinear model based FDI approaches for nonlinear systems (see for example [3], [4], [5], [6]), most FDI schemes have been based on linear time invariant (LTI) systems (e.g. [7], [8], [9]). Ad-hoc methods of gain scheduling to extend these linear methods to nonlinear systems, whilst attractive, do not guarantee the required level of performance, or even stability, other than at the points of design [10]. The same is also true for FDI schemes based on scheduled observers. A more formal natural extension of LTI based FDI approaches, is to consider LPV system based FDI (see for example [11], [12], [13], [14], [15]) to automatically schedule the observer or detection filter gains. This is a suitable compromise between 'full-blown' nonlinear designs such as [3], [4], [5], [6], and LTI methods based around an operating point. This allows the convenience associated with LTI schemes, and yet guarantees performance and stability over a wide operating envelope. A common application area for LPV systems is aerospace problems. Recent papers such as [16] demonstrate the successful application of an LPV detection filter to the longitudinal dynamics of a Boeing 747-100/200 aircraft. Although there is a wealth of literature on LPV based controller design (e.g. [17], [18], [19], [20], [10], [21]), the literature on LPV observer based FDI or LPV fault detection filters, is more limited. The work in [11], [13], [16], [12], [22], [23] and most recently [14], [15], [24], represents recent results in the field of LPV observer based FDI.

In the last decade there has been an explosion of interest in exploiting sliding mode techniques for FDI. The early sliding mode observer-based FDI papers built on traditional residual based FDI concepts (e.g. [25], [26]). The idea in [25], [26] was to ensure the sliding motion was broken when faults/failures occurred in the system. In practice, because of the robustness properties of sliding modes, this was difficult to realize. More recent work by [27], [28] focused on approaches which reconstruct/identify faults. Not only do these approaches detect and isolate the source of the faults/failures, they also provide additional insight about the faults/failures (e.g. shape and magnitude). This is advantageous and can be exploited for FTC: for example, the availability of a fault reconstruction signal means sensor faults can be corrected before the measurements are used by the controller (for example [29], [30]).

H. Alwi and C. Edwards are currently with the College of Engineering, Mathematics and Physical Sciences, University of Exeter, EX4 4QF, UK. h.alwi@exeter.ac.uk, C.Edwards@exeter.ac.uk

A. Marcos is currently with the Department of Aerospace Engineering, University of Bristol, BS8 1TR, UK. andres.marcos@bristol.ac.uk

Originally conceived in [31], the methods have evolved to include (Linear Matrix Inequality) LMI based design [32] and robustness to uncertainty [33]. In particular the method from [33] has recently been tested on an aircraft benchmark problem [30]. However the methods in [31], [32], [33] are based on LTI systems or quasi-linear systems [34] subject to uncertainty and thus are restricted to near trim conditions. One way to extend these methods to wider operating conditions is to introduce an LPV formulism. Although there are LPV based sliding mode control schemes (e.g. [35], [36]) proposed in the literature, there are no published LPV sliding mode observer schemes.

This paper proposes an extension of the schemes in [31] to a class of LPV systems. The LPV approach employed in this paper is motivated by the need to ensure the validity of the underlying model, about which the observer is designed, over a wide range of the flight envelope. In comparison with direct nonlinear approaches (e.g. [37]), the LPV model formulation is easier to obtain (e.g. through collections of linear models based on various flight conditions) and may explicitly contain models of the aerodynamic coefficients through polynomial fitting. This is a convenient way to capture the variations in the aerodynamic coefficients throughout the flight envelope to maintain a good fidelity level for the model. Also since the LPV approach can be thought of as a special case of gain scheduling, it can therefore be considered as a natural extension to linear based schemes and is widely accepted in the literature and industry. Therefore, an LPV methodology is suitable for the application considered in this paper: it has the convenience of a linear based approach while covering a wide range of the flight envelope with good fidelity as compared to nonlinear methods.

In this paper, both actuator and sensor faults are considered. For actuator faults, to extend the methods from [33] to LPV systems, and to achieve an observer regular form [31], it is assumed that the input distribution matrix associated with the faults, can be factorized into a fixed and varying part. The LPV observer design is based on a 'virtual system' formed from the factorized fixed distribution matrix, and the varying system matrices. In the case of sensor faults, the suggested design method involves re-formulating the problem as an actuator fault scenario. Therefore the observer design methodology for actuator FDI can also be used in these problems. The re-formulation is achieved by augmenting the original system with a filtered version of the faulty measurements. The augmentation considered in this paper differs from the one in [33] where the plant is augmented with filtered versions of *all* the outputs. Augmenting with only the potentially faulty measurements ensures the size of the augmented system is kept as low as possible. This is advantageous when employing the LMI synthesis.

The efficacy of the theoretical developments is demonstrated through its application to FDI scenarios in a benchmark aircraft problem from the literature [38], [39]. This benchmark was used as the basis for the GARTEUR AG-16 project aimed at demonstrating the benefits of modern FDI and FTC methods for aerospace systems. For actuator fault reconstruction, the example shows the practicality of the factorization of the input distribution matrix associated with the actuators to be monitored, and the design procedure for the observer gains. The proposed observer scheme is tested on the full nonlinear high fidelity model of the aircraft [40]. To demonstrate sensor fault reconstruction, the same example is considered. In both situations, the results show successful reconstruction of faults.

II. Actuator fault reconstruction for LPV systems

A. LPV system description

Consider an LPV plant subject to actuator faults represented by

$$\dot{x}(t) = A(\rho)x(t) + B(\rho)u(t) + D(\rho)f_i(t) \quad (1)$$

$$y(t) = Cx(t) \quad (2)$$

where $A(\rho) \in \mathbb{R}^{n\times n}, B(\rho) \in \mathbb{R}^{n\times m}, D(\rho) \in \mathbb{R}^{n\times q}$ are parameter varying matrices, and the matrix $C \in \mathbb{R}^{p\times n}$ is fixed. The dimensions representing the state order, the number of measured outputs and the number of independent faults are assumed to satisfy $n > p \geq q$. It is assumed that the inputs $u(t)$ and the outputs $y(t)$ are available for the FDI scheme. The unknown signal $f_i(t) : \mathbb{R}^+ \to \mathbb{R}^q$ represents the effect of the faults. In fault–free conditions $f_i = 0$, but when $f_i \neq 0$, a fault exists in the system. Assume that the varying parameters, $\rho \in \Omega \subset \mathbb{R}^d$, where Ω is a compact set. Furthermore assume ρ is available (i.e. perfectly measurable) for the observer scheme which will be proposed.

Assume the varying matrix $D(\rho)$ can be factorized into a fixed and a varying component

$$D(\rho) = DE(\rho) \quad (3)$$

where $D \in \mathbb{R}^{n\times q}$, and $E(\rho) \in \mathbb{R}^{q\times q}$. It is assumed $E(\rho)$ is invertible for all $\rho \in \Omega$. This will assist in the development of the observer, and will be discussed later. Although this is clearly a restriction, this perfect factorization is quite common for over actuated systems or systems with redundancy e.g. large civil aircraft [40], [41]. An example of just such a factorization for a large civil aircraft will be shown later in the paper.

Using (3), the system in (1) can be re-written as

$$\dot{x}(t) = A(\rho)x(t) + B(\rho)u(t) + D\underbrace{E(\rho)f_i(t)}_{f_\nu(t,\rho)} \tag{4}$$

where the function $f_\nu(t,\rho) : \mathbb{R}_+ \times \mathbb{R}^d \to \mathbb{R}^q$ now represents the unknown 'virtual faults' which will be estimated by the observer. However, because $\det(E(\rho)) \neq 0$, the actual fault $f_i(t)$ can be estimated once estimates of $f_\nu(t,\rho)$ are available. Assume that

$$\|f_\nu(t,\rho)\| < r_1(\rho)\|u\| + \varphi(t,y,\rho) \tag{5}$$

where $r_1(\rho)$ and $\varphi : \mathbb{R}_+ \times \mathbb{R}^p \times \mathbb{R}^d \to \mathbb{R}_+$ are known functions and y is the measured output from (2). Equation (5) constitutes an upper bound on the worse case effect of the fault impacting on the model dynamics.

B. LPV sliding mode observer

The proposed observer has the structure

$$\dot{\hat{x}}(t) = A(\rho)\hat{x}(t) + B(\rho)u(t) - G_l(\rho)e_y(t) + G_n\nu(t) \tag{6}$$

where the gains $G_l(\rho) \in \mathbb{R}^{n\times p}$ and $G_n \in \mathbb{R}^{n\times p}$ are the design freedom to be exploited to induce a sliding motion [31]. The objective is to force the output estimation error

$$e_y(t) = \hat{y}(t) - y(t) \tag{7}$$

to zero in finite time where $\hat{y}(t) = C\hat{e}(t)$. Once the output error is zero, a first order sliding mode is said to have been attained [42] on the surface

$$\mathcal{S} = \{e \in \mathbb{R}^n : Ce = 0\} \tag{8}$$

where $e(t) = \hat{x}(t) - x(t)$ is the state estimation error. During sliding, actuator faults can be estimated using the 'equivalent output injection' [42], [31], [32], [33] signals required to maintain sliding.

From the definition of e, subtracting (6) from (4) yields the error system

$$\dot{e}(t) = A(\rho)e(t) - G_l(\rho)e_y(t) + G_n\nu(t) - Df_\nu(t,\rho) \tag{9}$$

In order to obtain the 'observer regular form', the following key assumption is made:

Assumption 1: $\text{rank}(CD) = q$ where C and D are defined in (1) and (3).

Since D is a fixed matrix and CD is full rank, there exists a coordinate transformation [31] $x(t) \mapsto T_o x(t)$ such that

$$y(t) = \underbrace{\begin{bmatrix} 0 & T \end{bmatrix}}_{C} \begin{bmatrix} x_1(t) \\ x_2(t) \end{bmatrix} \tag{10}$$

and the fault distribution matrix

$$D = \begin{bmatrix} \frac{0}{D_2} \end{bmatrix} = \begin{bmatrix} \frac{0}{0} \\ D_o \end{bmatrix} \tag{11}$$

where $T \in \mathbb{R}^{p\times p}$ and is orthogonal, and $D_2 \in \mathbb{R}^{p\times q}$, and $D_o \in \mathbb{R}^{q\times q}$ is nonsingular. In this observer regular form, the error system (9) can be written as

$$\begin{bmatrix} \dot{e}_1(t) \\ \dot{e}_2(t) \end{bmatrix} = \underbrace{\begin{bmatrix} A_{11}(\rho) & A_{12}(\rho) \\ A_{21}(\rho) & A_{22}(\rho) \end{bmatrix}}_{A(\rho)} \begin{bmatrix} e_1(t) \\ e_2(t) \end{bmatrix} - \underbrace{\begin{bmatrix} 0 \\ D_2 \end{bmatrix}}_{D} f_\nu(t,\rho) - \begin{bmatrix} G_{l_1}(\rho) \\ G_{l_2}(\rho) \end{bmatrix} e_y(t) + \begin{bmatrix} G_{n_1} \\ G_{n_2} \end{bmatrix} \nu(t) \tag{12}$$

where $e_1 \in \mathbb{R}^{n-p}$ and $e_2 \in \mathbb{R}^p$. Consider a further state transformation

$$\tilde{e}(t) = \begin{bmatrix} \tilde{e}_1(t) \\ e_y(t) \end{bmatrix} = T_L \begin{bmatrix} e_1(t) \\ e_2(t) \end{bmatrix} = \begin{bmatrix} e_1(t) + Le_y(t) \\ e_y(t) \end{bmatrix} \tag{13}$$

where $T_L \in \mathbb{R}^{n\times n}$ is given by

$$T_L = \begin{bmatrix} I & L \\ 0 & T \end{bmatrix} \tag{14}$$

and $L \in \mathbb{R}^{(n-p)\times p}$. The matrix L represents the design freedom. In the new coordinates $\tilde{e}$, the output distribution matrix

$$e_y(t) = \underbrace{\begin{bmatrix} 0 & I \end{bmatrix}}_{\tilde{C}} \tilde{e}(t) \tag{15}$$

As in [33], the matrix L is assumed to have the special structure

$$L = \begin{bmatrix} L_1 & 0 \end{bmatrix} \tag{16}$$

where $L_1 \in \mathbb{R}^{(n-p)\times(p-q)}$. In the new coordinates, the gain associated with the nonlinear injection is chosen as

$$\tilde{G}_n = T_L G_n = \begin{bmatrix} 0 \\ I_p \end{bmatrix} \tag{17}$$

and the error system from (12) can be written in the new coordinates as

$$\begin{bmatrix} \dot{\tilde{e}}_1(t) \\ \dot{e}_y(t) \end{bmatrix} = \underbrace{\begin{bmatrix} \tilde{A}_{11}(\rho) & \tilde{A}_{12}(\rho) \\ \tilde{A}_{21}(\rho) & \tilde{A}_{22}(\rho) \end{bmatrix}}_{\tilde{A}(\rho)=T_L A(\rho) T_L^{-1}} \begin{bmatrix} \tilde{e}_1(t) \\ e_y(t) \end{bmatrix} - \underbrace{\begin{bmatrix} 0 \\ \tilde{D}_2 \end{bmatrix}}_{\tilde{D}=T_L D} f_\nu(t,\rho) - \underbrace{\begin{bmatrix} \tilde{G}_{l_1}(\rho) \\ \tilde{G}_{l_2}(\rho) \end{bmatrix}}_{\tilde{G}_l(\rho)} e_y(t) + \underbrace{\begin{bmatrix} 0 \\ I \end{bmatrix}}_{\tilde{G}_n} \nu(t) \tag{18}$$

where the fact that $LD_2 = 0$ has been used to obtain the above (because of the structures of D and L in (11) and (16)). In (18), by definition, $\tilde{D}_2 = TD_2$ and

$$e_y(t) = \tilde{C}\tilde{e}(t) = \begin{bmatrix} 0 & I_p \end{bmatrix} \tilde{e}(t)$$

Furthermore

$$\tilde{A}(\rho) = \begin{bmatrix} \tilde{A}_{11}(\rho) & \tilde{A}_{12}(\rho) \\ \tilde{A}_{21}(\rho) & \tilde{A}_{22}(\rho) \end{bmatrix} = \begin{bmatrix} A_{11}(\rho) + LA_{21}(\rho) & A_{12}(\rho)T^{-1} + LA_{22}(\rho)T^{-1} - \tilde{A}_{11}(\rho)LT^{-1} \\ TA_{21}(\rho) & TA_{22}(\rho)T^{-1} - TA_{21}(\rho)LT^{-1} \end{bmatrix} \tag{19}$$

Due to the special structure of L from (16), the top left sub-block of (19) is

$$\tilde{A}_{11}(\rho) = A_{11}(\rho) + L_1 A_{211}(\rho) \tag{20}$$

where $A_{211}(\rho) \in \mathbb{R}^{(p-q)\times(n-p)}$ represents the top $(p-q)$ rows of $A_{21}(\rho)$ in (12). Suppose a matrix L_1 can be chosen such that $\tilde{A}_{11}(\rho)$ is quadratically stable i.e. there exists a symmetric positive definite (s.p.d) matrix $P_1 \in \mathbb{R}^{(n-p)\times(n-p)}$ and an $L_1 \in \mathbb{R}^{(n-p)\times(p-q)}$ such that

$$\tilde{A}_{11}(\rho)^{\mathrm{T}} P_1 + P_1 \tilde{A}_{11}(\rho) < 0 \tag{21}$$

for all $\rho \in \Omega$. A choice of observer gain $\tilde{G}_l(\rho)$ from (18) is then

$$\tilde{G}_l(\rho) = \begin{bmatrix} \tilde{G}_{l_1}(\rho) \\ \tilde{G}_{l_2}(\rho) \end{bmatrix} = \begin{bmatrix} \tilde{A}_{12}(\rho) \\ \tilde{A}_{22}(\rho) - \tilde{A}_{22}^s \end{bmatrix} \tag{22}$$

where

$$\tilde{A}_{22}^s = -k_2 I_p \tag{23}$$

and k_2 is a positive design scalar. Substituting (22) into (18) yields

$$\begin{bmatrix} \dot{\tilde{e}}_1(t) \\ \dot{e}_y(t) \end{bmatrix} = \begin{bmatrix} \tilde{A}_{11}(\rho) & 0 \\ \tilde{A}_{21}(\rho) & -k_2 I_p \end{bmatrix} \begin{bmatrix} \tilde{e}_1(t) \\ e_y(t) \end{bmatrix} - \begin{bmatrix} 0 \\ \tilde{D}_2 \end{bmatrix} f_\nu(t,\rho) + \begin{bmatrix} 0 \\ I \end{bmatrix} \nu(t) \tag{24}$$

For the injection term $\nu \in \mathbb{R}^p$, consider the jth component $\nu_j(t)$ defined by

$$\nu_j(t) = -k_1 \text{sign}(e_{y,j}(t)) |e_{y,j}(t)|^{1/2} + z_j(t) \tag{25}$$
$$\dot{z}_j(t) = -k_3 \text{sign}(e_{y,j}(t)) - k_4 e_{y,j}(t) \tag{26}$$

for $j = 1, 2, \ldots p$ where $e_y = \text{col}(e_{y,1}, e_{y,2} \ldots e_{y,p})$. The variables k_1, k_3, k_4 (and k_2) are design scalars to be chosen. The lower equations from (24) together with (25) can be written component-wise as

$$\dot{e}_{y,j}(t) = \tilde{\xi}_j(t) - k_2 e_{y,j}(t) - \tilde{D}_{2,j} f_\nu(t,\rho) + \nu_j(t) \tag{27}$$

where $\tilde{D}_{2,j}$ is the jth row of $\tilde{D}_2$ and

$$\tilde{\xi}_j(t) = \tilde{A}_{21,j}(\rho) \tilde{e}_1(t) \tag{28}$$

where $\tilde{A}_{21,j}(\rho)$ is the jth row of the varying matrix $\tilde{A}_{21}(\rho)$ from (24). Consequently combining (25)-(27) yields

$$\dot{e}_{y,j}(t) = -k_1 \,\text{sign}(e_{y,j}(t)) |e_{y,j}(t)|^{1/2} - k_2 \, e_{y,j}(t) + z_j(t) + \tilde{\xi}_j(t) - \tilde{D}_{2,j} f_\nu(t,\rho) \tag{29}$$
$$\dot{z}_j(t) = -k_3 \,\text{sign}(e_{y,j}(t)) - k_4 \, e_{y,j}(t) \tag{30}$$

for $j = 1, 2, \ldots p$. Making the change of variable

$$\tilde{z}_j(t) := z_j(t) + \tilde{\xi}_j(t) - \tilde{D}_{2,j} f_\nu(t,\rho) \tag{31}$$

Equations (29)-(30) can be re-written as

$$\dot{e}_{y,j}(t) = -k_1 \,\text{sign}(e_{y,j}(t)) |e_{y,j}(t)|^{1/2} - k_2 \, e_{y,j}(t) + \tilde{z}_j(t) \tag{32}$$
$$\dot{\tilde{z}}_j(t) = -k_3 \,\text{sign}(e_{y,j}(t)) - k_4 \, e_{y,j}(t) + \phi_i(t) \tag{33}$$

where $\phi_i(t) = \dot{\tilde{\xi}}_j(t) - \tilde{D}_{2,j} \dot{f}_\nu(t,\rho)$. Furthermore

$$|\phi_i(t)| < \|\dot{\tilde{\xi}}_j(t)\| + \|\tilde{D}_{2,j}\| \, \|\dot{f}_\nu(t,\rho)\| \tag{34}$$
$$\leq \|\frac{\partial \tilde{A}_{21,j}}{\partial \rho}\| \, \|\dot{\rho}\| \, \|\tilde{e}_1(t)\| + \|\tilde{A}_{21,j}\| \, \|\dot{\tilde{e}}_1(t)\| + \|\tilde{D}_{2,j}\| \, \|\dot{f}_\nu(t,\rho)\| \tag{35}$$

Then since the autonomous system associated with the states $\tilde{e}_1(t)$ in (24) is stable, $\|\tilde{e}_1\|$ and $\|\dot{\tilde{e}}_1\|$ are bounded. Provided $\|\dot{f}_\nu(t,\rho)\|$ is bounded, $\tilde{A}_{21}(\rho)$ is affine in ρ and the LPV parameter changes are bounded (i.e. $\dot{\rho}$ is bounded), then it follows $|\phi_i(t)| < \varepsilon$ for some sufficiently large ε. Note that (32)-(33) is a special case of the supertwisting structure from [43]. As in [43] the gains from (32) and (33) are chosen as

$$k_1 > 2\sqrt{\varepsilon} \tag{36}$$
$$k_2 > 0 \tag{37}$$
$$k_3 > \varepsilon \tag{38}$$
$$k_4 > \frac{(k_2)^2 \left((k_1)^3 + \frac{5}{4}(k_1)^2 + \frac{5}{2}(k_3 - \varepsilon) \right)}{k_1 (k_3 - \varepsilon)} \tag{39}$$

Consequently from the results in [43], $e_{y,j} = \dot{e}_{y,j} = 0$ in finite time. Therefore from (32), $\tilde{z}_j(t) = 0$ in finite time and from the definition of $\tilde{z}_j(t)$ in (31),

$$z_j(t) = \tilde{D}_{2,j} f_\nu(t,\rho) - \tilde{\xi}_j(t) \tag{40}$$

in finite time. From (24), $\dot{\tilde{e}}_1 = \tilde{A}_{11}(\rho)\tilde{e}_1$ and since by construction $\tilde{A}_{11}(\rho)$ is quadratically stable, $\tilde{e}_1(t) \to 0$. Therefore from (28) and (40)

$$z(t) \to \tilde{D}_2 f_\nu(t,\rho) \tag{41}$$

asymptotically where $z(t) = [z_1, z_2 \ldots, z_p]^{\mathrm{T}}$ is from (26). Therefore the output fault $f_\nu(t,\rho)$ can be reconstructed online using the expression

$$\hat{f}_\nu(t) = \tilde{D}_2^\dagger z(t) \tag{42}$$

where $\tilde{D}_2^\dagger$ is the pseudo inverse of the matrix $\tilde{D}_2$ since by assumption $\tilde{D}_2$ is full column rank. By assumption $E(\rho)$ is invertible and using (4), the actual actuator fault can be estimated as

$$\hat{f}_i(t) = E(\rho)^{-1}\hat{f}_\nu(t) \tag{43}$$

Using (42), an estimate of the fault can be written as

$$\hat{f}_i(t) = \underbrace{E(\rho)^{-1}}_{varying}\ \underbrace{\tilde{D}_2^\dagger}_{fixed}\ z(t) \tag{44}$$

where one potential choice for $\tilde{D}_2^\dagger = (\tilde{D}_2^T\tilde{D}_2)^{1-}\tilde{D}_2^T$. Note that the inverse in this expression is well defined, since $\tilde{D}_2$ has full column rank by construction.

Remark: During the sliding motion once the reduced order dynamics have disappeared, the fault $f_\nu(t,\rho)$ is related to $z(t)$ through

$$z(t) = \tilde{D}_2 f_\nu(t,\rho) \tag{45}$$

Substituting for $z(t)$ from (45) into (42), and using the expression for $\tilde{D}_2^\dagger$ given above, ensures $\hat{f}_\nu = f_\nu$. In the case when the reduced order dynamics are still decaying, and $z(t) \approx \tilde{D}_2 f_\nu(t,\rho)$, a least squares solution will be obtained.

III. Sensor fault reconstruction for LPV systems

A. LPV system with sensor faults

For the sensor fault reconstruction problem, consider an LPV plant represented by

$$\dot{x}(t) = A(\rho)x(t) + B(\rho)u(t) \tag{46}$$

$$y(t) = Cx(t) + Nf_o(t) \tag{47}$$

where $f_o(t) \in \mathbb{R}^r$ is the (unknown) vector of sensor faults and $N \in \mathbb{R}^{p\times r}$ where $\mathrm{rank}(N) = r$ and $r \le p$. This corresponds to a scenario in which some of the sensors are fault-free while some are prone to faults. In Engineering systems this is not an unreasonable assumption - some sensors may be inherently less reliable or more vulnerable to external damage or else constitute the output from some triplex voting system [44]. Typically the columns of N correspond to the standard basis for $\mathbb{R}^p$. In this situation by permutating the order of the outputs, without loss of generality assume that the plant representation is in a form where the outputs which are prone to faults are in the lower output equations, i.e.

$$y(t) = \left[\begin{array}{c} y_1(t) \\ \hline y_2(t) \end{array}\right] \begin{array}{l} \}\text{fault free} \\ \}\text{prone to fault} \end{array} = \underbrace{\left[\begin{array}{c} C_1 \\ \hline C_2 \end{array}\right]}_{C} x(t) + \underbrace{\left[\begin{array}{c} 0 \\ \hline I \end{array}\right]}_{N} f_o(t) \tag{48}$$

where $C_1 \in \mathbb{R}^{(p-r)\times n}$, and $C_2 \in \mathbb{R}^{r\times n}$.

The idea now is to re-formulate the problem such that the fault reconstruction scheme in Section II can be used to estimate $f_o(t)$. Consider a new state $z_f(t) \in \mathbb{R}^r$ which is the filtered output of $y_2(t)$: specifically

$$\dot{z}_f(t) = -A_f z_f(t) + A_f y_2(t) \tag{49}$$

where $-A_f$ is a stable matrix of dimension $\mathbb{R}^{r\times r}$. Substituting for $y_2(t)$ from (48) into (49) and augmenting with system (46) yields

$$\underbrace{\left[\begin{array}{c} \dot{x}(t) \\ \dot{z}_f(t) \end{array}\right]}_{\dot{x}_a} = \underbrace{\left[\begin{array}{cc} A(\rho) & 0 \\ A_f C_2 & -A_f \end{array}\right]}_{A_a(\rho)} \underbrace{\left[\begin{array}{c} x(t) \\ z_f(t) \end{array}\right]}_{x_a} + \underbrace{\left[\begin{array}{c} B(\rho) \\ 0 \end{array}\right]}_{B_a(\rho)} u(t) + \underbrace{\left[\begin{array}{c} 0 \\ A_f \end{array}\right]}_{F_a} f_o(t) \tag{50}$$

Replacing the system output $y_2(t)$ from (48), with the filtered version in (49), generates a new 'output' (of the augmented system) with the form

$$\underbrace{\begin{bmatrix} y_1(t) \\ z_f(t) \end{bmatrix}}_{y_a} = \underbrace{\begin{bmatrix} C_1 & 0 \\ 0 & I_r \end{bmatrix}}_{C_a} \underbrace{\begin{bmatrix} x(t) \\ z_f(t) \end{bmatrix}}_{x_a} \tag{51}$$

Note that this augmentation scheme is different from the one originally proposed in [33] where the system is augmented with all the filtered outputs of the plant. Now the output (51) is a combination of the actual and the filtered outputs (which are prone to faults). System (50)-(51) is in the form of (4), and an observer can be designed by replacing $(A(\rho), D, C)$ in (9) and (7) with $(A_a(\rho), F_a, C_a)$ in (50) and (51) respectively. By construction, rank$(C_aF_a) = r$ where C_a and F_a are defined in (51) and (50).

A further change of coordinates is required to ensure that the augmented system outputs are in the form in (15). To achieve this, consider a coordinate transformation $x_a \mapsto T_{o_{aug}} x_a = \hat{x}_a$ where

$$\underbrace{\begin{bmatrix} \hat{x}(t) \\ z_f(t) \end{bmatrix}}_{\hat{x}_a} = \underbrace{\begin{bmatrix} T_s & 0 \\ 0 & I_r \end{bmatrix}}_{T_{oaug}} \underbrace{\begin{bmatrix} x(t) \\ z_f(t) \end{bmatrix}}_{x_a} = \begin{bmatrix} T_s x(t) \\ z_f(t) \end{bmatrix} \tag{52}$$

and $T_s \in \mathbb{R}^{n\times n}$ is any nonsingular matrix such that $C_1 T_s^{-1} = \begin{bmatrix} 0 & I_{p-r} \end{bmatrix}$. Then, in the new coordinates

$$\hat{C}_a = \underbrace{\begin{bmatrix} C_1 & 0 \\ 0 & I_r \end{bmatrix}}_{C_a} \underbrace{\begin{bmatrix} T_s & 0 \\ 0 & I_r \end{bmatrix}}_{T_{o_{aug}}^{-1}} = \begin{bmatrix} C_1 T_s^{-1} & 0 \\ 0 & I_r \end{bmatrix} = \begin{bmatrix} \begin{bmatrix} 0 & I_{p-r} \end{bmatrix} & 0 \\ 0 & I_r \end{bmatrix} = \begin{bmatrix} 0 & I_p \end{bmatrix} \tag{53}$$

and the augmented system in (50) becomes

$$\dot{\hat{x}}_a = \hat{A}_a(\rho) x_a(t) + \hat{B}_a(\rho) u(t) + \hat{F}_a f_o(t) \tag{54}$$

where

$$\hat{A}_a(\rho) = \begin{bmatrix} T_s A(\rho) T_s^{-1} & 0 \\ A_f C_2 T_s^{-1} & -A_f \end{bmatrix}, \hat{B}_a(\rho) = \begin{bmatrix} T_s B(\rho) \\ 0 \end{bmatrix}, \hat{F}_a = \begin{bmatrix} 0 \\ A_f \end{bmatrix} \tag{55}$$

Note that the system described in (53)-(55) above, is in the regular form similar to (10)-(12). Therefore the observer design synthesis in Section II-B can also be used here.

IV. Actuator fault reconstruction example

This section describes an application of the new theory described in the earlier sections to an aerospace system benchmark FTLAB747. The FTLAB747 software running under Matlab has been developed for the study of fault tolerant control and FDI schemes. It represents a 'real world' model of a B747-100/200 aircraft. The technical data and the underlying differential equations were originally obtained from NASA [38], [39], and the software was developed at Delft University of Technology by van der Linden (Delft University Aircraft Simulation and Analysis Tool, DASMAT) [45]. It was subsequently upgraded by Smaili (FTLAB747) [46] and used in the independent investigation of the Bijlmermeer incident [47] by Delft University of Technology [48]. The software was later enhanced by Marcos and Balas [40] (FTLAB747 V6.1/V6.5) and used as a testing platform for fault detection and fault tolerant control schemes. The high fidelity nonlinear model has 77 states incorporating rigid body variables, sensors, actuators and aero-engine dynamics. All the control surfaces and engine dynamics are highly detailed and comprise dynamics with hard nonlinearities for actuator position and rate limits. The capabilities of this software as a realistic platform to test FTC and FDI schemes is demonstrated by its subsequent use by many researchers (see for example references [49], [50], [7], [16], [51]). More recently this software has been upgraded by Smaili *et al.*[52] and used as a generic test bed for the GARTEUR AG16 group [41] which studied and compared state of the art fault detection and fault tolerant control schemes. The LPV plant used as a basis for the observer design has been obtained from [53] (which is derived from the FTLAB747). The LPV plant was created using the function substitution LPV modelling approach [54], where the aerodynamic coefficients from [38], [39] have been simplified

by polynomial fitting. The aerodynamic coefficients are polynomial functions of velocity (V_{tas}) and angle of attack (α) for the range of [150, 250]m/s and [-2, 8]$^\circ$ respectively, at a fixed altitude of 7000m [53]. The LPV system states and inputs are deviations from the trim values (i.e. $\bar{x} = x - x_{trim}$ and $\bar{u} = u - u_{trim}$). Further details of the LPV model description, trim values, and a validation of the LPV model can be found in [53], [54].

The states of the LPV plant in [53] are $[\bar{\alpha},\ \bar{q},\ \bar{V}_{tas},\ \bar{\theta},\ \bar{h}_e]^{\mathrm{T}}$ (which represent angle of attack, pitch rate, speed, pitch and altitude) and the inputs are $[\bar{\delta}_e,\ \bar{\delta}_s,\ \bar{T}_n]$ (which represent elevator, stabilizer and thrust). In this example, the outputs of the LPV plant are $[\bar{V}_{tas},\ \bar{\alpha},\ \bar{q}]^{\mathrm{T}}$. The LPV system given in [53] is obtained at trim values of

$$[\alpha_{trim},\ q_{trim},\ V_{tas_{trim}},\ \theta_{trim},\ h_{e_{trim}}] = [1.05^\circ,\ 0^\circ/s,\ 227.02m/s,\ 1.05^\circ,\ 7000m]$$

$$[\delta_{e_{trim}},\ \delta_{s_{trim}},\ T_{n_{trim}}] = [0.163^\circ,\ 0.590^\circ,\ 42291N]$$

The states have been reordered and $\bar{h}_e$ has been removed so that for design purposes the state vector becomes $[\bar{\theta},\ \bar{V}_{tas},\ \bar{\alpha},\ \bar{q}]^{\mathrm{T}}$ with inputs $[\bar{\delta}_e,\ \bar{\delta}_s,\ \bar{T}_n]$. The LPV system matrices are given by

$$A(\rho) = A_0 + \sum_{i=1}^{7} A_i \rho_i \tag{56}$$

$$B(\rho) = B_0 + \sum_{i=1}^{7} B_i \rho_i \tag{57}$$

where

$$[\rho_1,\ \rho_2,\ \rho_3,\ \rho_4,\ \rho_5,\ \rho_6,\ \rho_7] := [\bar{\alpha},\ \bar{V}_{tas},\ \bar{V}_{tas}\bar{\alpha},\ \bar{V}_{tas}^2,\ \bar{V}_{tas}^2\bar{\alpha},\ \bar{V}_{tas}^3,\ \bar{V}_{tas}^4] \tag{58}$$

and $\bar{\alpha} = \alpha - \alpha_{trim},\ \bar{V}_{tas} = V_{tas} - V_{tas_{trim}}$. Details of the matrices A_i, B_i for $i = 1, \ldots 7$ are given in the Appendix, and the output distribution matrix is given by

$$C = \begin{bmatrix} 0 & I_3 \end{bmatrix}$$

In regular form, the LPV input distribution matrix is given by

$$B(\rho) = \begin{bmatrix} 0 & 0 & 0 \\ 0 & 0 & B_{23}(\rho) \\ B_{31}(\rho) & B_{32}(\rho) & B_{33}(\rho) \\ B_{41}(\rho) & B_{42}(\rho) & B_{43}(\rho) \end{bmatrix} \tag{59}$$

Here, it is assumed that the engines are fault free. The actuators that will be monitored for faults are the elevator and stabilizer. Therefore the fault distribution matrix $D(\rho)$ from (1) is given by

$$D(\rho) = \begin{bmatrix} 0 & 0 \\ 0 & 0 \\ B_{31}(\rho) & B_{32}(\rho) \\ B_{41}(\rho) & B_{42}(\rho) \end{bmatrix} \tag{60}$$

i.e. the first two columns of $B(\rho)$ in (59). The key observation is that the matrix $D(\rho)$ in (60) can be factorized as in (3) where

$$D(\rho) = \underbrace{\begin{bmatrix} 0 & 0 \\ 0 & 0 \\ 1 & 0 \\ 0 & 1 \end{bmatrix}}_{D} \underbrace{\begin{bmatrix} B_{31}(\rho) & B_{32}(\rho) \\ B_{41}(\rho) & B_{42}(\rho) \end{bmatrix}}_{E(\rho)} \tag{61}$$

It is clear that rank$(CD) = 2$ (i.e. full rank) and all the theory developed in the earlier sections can now be applied.

A. LPV Observer Design

The design of the observer gains in (6) are dependent on L_1 as shown in (17), (22), (16) and (14). The design freedom matrix L_1 can be synthesized from an LMI perspective using the single quadratic Lyapunov function approach [17] according to

$$(A_{11}(\rho) + L_1 A_{211}(\rho))^{\mathrm{T}} P_1 + P_1 (A_{11}(\rho) + L_1 A_{211}(\rho)) < 0 \tag{62}$$

$$P_1 > 0 \tag{63}$$

The solution for P_1 and the design gain L_1 are obtained as part of the output of the standard MATLAB LMI multi-model state feedback synthesis code 'msfsyn' [55] adapted to tackle an observer problem (i.e. the dual of the standard control problem). Here, a regional pole placement design [55] has been selected to place the closed-loop poles inside specific LMI regions [55], [56] in the complex plane to the left of the vertical line through -1. Using 'msfsyn' [55] this yields $L_1 = 1.1476$ with $P_1 = 1.1738 \times 10^{-7}$. The range of V_{tas} and α is given by $[150,\ 250]$m/s and $[-2,\ 8]^\circ$ respectively [53]. The stable design matrix $\tilde{A}^s_{22}$ from (23) has been chosen as $\tilde{A}^s_{22} = -I_3$ where $k_3 = 1$. It can be shown the fixed gain $\tilde{G}_n$ in (17) can be written in the original coordinates as $G_n = T_o^{-1} T_L^{-1} \tilde{G}_n$ and is given by

$$G_n = \begin{bmatrix} -1.1476 & 0 & 0 \\ 1 & 0 & 0 \\ 0 & 1 & 0 \\ 0 & 0 & 1 \end{bmatrix}$$

For simulation, the gain $\tilde{G}_l(\rho)$ in (22) has been split into varying and fixed components and written in the original coordinates as

$$G_l(\rho) = T_o^{-1} T_L^{-1} \tilde{G}_l(\rho) = T_o^{-1} T_L^{-1} \left(\begin{bmatrix} \tilde{A}_{12}(\rho) \\ \tilde{A}_{22}(\rho) \end{bmatrix} - \begin{bmatrix} 0 \\ \tilde{A}^s_{22} \end{bmatrix} \right) = G_{la}(\rho) - G_{lb}$$

where

$$G_{lb} = \begin{bmatrix} 1.1476 & 0 & 0 \\ -1 & 0 & 0 \\ 0 & -1 & 0 \\ 0 & 0 & -1 \end{bmatrix}$$

while

$$G_{la}(\rho) = G_{la_0} + \sum_{i=1}^{7} G_{la_i} \rho_i$$

See the Appendix for details about the individual gains. The individual gains for the 'output injection signal' and the linear gains in (23), (25) and (26) are $k_1 = 2.1, k_2 = 1, k_3 = 2$ and $k_4 = 9.0480$.

Remark: Note that for the LPV system considered here, the matrix $\tilde{A}_{21}(\rho)$ from (19) is fixed. Therefore (34) and (35) can be re-written as

$$\begin{aligned} |\phi_i(t)| &< \|\dot{\tilde{\xi}}_j(t)\| + \|\tilde{D}_{2,j}\| \, \|\dot{f}_\nu(t,\rho)\| \\ &\leq \|\tilde{A}_{21,j}\| \, \|\dot{\tilde{e}}_1(t)\| + \|\tilde{D}_{2,j}\| \, \|\dot{f}_\nu(t,\rho)\| \end{aligned} \tag{64}$$

In this case, the bound on $|\phi_i(t)|$ only depends on the bound of $\|\dot{f}_\nu(t,\rho)\|$. Here it was found that choosing $\varepsilon = 1$ was a suitable choice.

Remark: In this example the chosen outputs were $[\bar{V}_{tas},\ \bar{\alpha},\ \bar{q}]^{\mathrm{T}}$ which means that the CD full rank condition was satisfied. If instead $[\bar{V}_{tas},\ \bar{\alpha},\ \bar{\theta}]^{\mathrm{T}}$ were the chosen outputs, it can be verified following the procedure given earlier that rank$(CD) = 1$ and the assumptions are not satisfied since the relative degree one condition has been lost. However, using the approach proposed in [57], a supertwist differentiator could be used in conjunction with $\bar{\theta}$ to create in real-time a signal $\frac{d\bar{\theta}}{dt}$ and the approach described in Section II could still be employed – even in this relative degree two situation.

B. Actuator Faults Reconstruction Results

A closed-loop controller has been used to provide a simulation environment in which altitude is maintained (since the LPV model assumes a fixed altitude). The controller also ensures a good response to a change in speed. The controller associated with all the results in this paper is based on the reconfigurable LPV control design [21] for the longitudinal axis, which is the baseline controller given in the FTLAB747-V6.1/6.5 software and is described in detail in [21]. The controlled outputs are flight path angle (γ) and speed. The controller uses the elevators and thrust for flight manoeuvres, while the stabilizer is used to trim the aircraft [21]. The controller was originally designed to deal with elevator faults and failures. The faults in this paper are simulated as additive perturbations occurring in the actuator inputs. This facilitates the analysis of the performance of the fault reconstruction scheme. Such an approach is also considered in [16] for example.

The nonlinear simulations were conducted using the FTLAB747-V6.1/6.5 software which runs under MATLAB and SIMULINK. The nonlinear simulation was conducted with trim conditions of

$$[\alpha_{trim},\ q_{trim},\ V_{tas_{trim}},\ \theta_{trim},\ h_{e_{trim}}]^{\mathrm{T}} = [1.8^\circ,\ 0^\circ/s,\ 227.02m/s,\ 1.8^\circ,\ 7000m]$$

$$[\delta_{e_{trim}},\ \delta_{s_{trim}},\ T_{n_{trim}}] = [0.5895^\circ,\ 0.0591^\circ,\ 40863N]$$

Note that these are not exactly the same trim values used to obtain the LPV model in [53]. This is due to the fact that some of the trim configurations are not available in [53] (e.g. the initial mass and the x_{cg} location). The above trim was obtained with an initial mass of 300,000kg, $x_{cg} = 25\%mac$ and 1.085° pilot column deflection.

Figure 1 shows the simulation results from using the nonlinear plant in an elevator fault scenario. The faults are simulated as additive perturbations at the actuator command from the controller (as shown in Figure 1(c)) and are unknown to the observer. Note that sensor noise is considered in the FTLAB747-V6.1/6.5 software simulation package. The sensor noise considered is Gaussian noise with variance ranges from 1×10^{-2} to 1×10^{-8} depending on the particular channel. The effect of noise can be seen in Figures 1(a) and 1(b). Figure 1(a) shows the demanded change in speed and the speed tracking performance. There is a zero demand on γ (to maintain altitude at 7000m). Figure 1(a) shows good tracking performance even in the presence of the elevator fault. Figure 1(b) shows that the controller (u_e) has managed to compensate for the additive fault which does not appear in the elevator deflection δ_e. Figure 1(c) shows good reconstruction of the fault by the proposed observer scheme.

V. SENSOR FAULTS RECONSTRUCTION EXAMPLE

As in Section IV-B, the simulations associated with the sensor fault reconstruction are from the full high-fidelity nonlinear model using FTLAB747. In this example, it will be assumed that only the θ measurement is prone to faults. The system states have been reordered as $x(t) = [\alpha,\ q,\ V_{tas},\ \theta]$, so that

$$y(t) = \left.\begin{bmatrix} \alpha(t) \\ q(t) \\ \hline V_{tas}(t) \\ \theta(t) \end{bmatrix}\right\}\begin{matrix}\text{fault free} \\ \\ \text{prone to fault}\end{matrix} = C_1\left\{\underbrace{\left[\begin{array}{cccc} 1 & 0 & 0 & 0 \\ 0 & 1 & 0 & 0 \\ 0 & 0 & 1 & 0 \end{array}\right]}_{C_1}\right. x(t) + \underbrace{\begin{bmatrix} 0 \\ 0 \\ 0 \end{bmatrix}}_{N_1} F_o(t)$$

$$C_2\left\{\underbrace{\left[\begin{array}{cccc} 0 & 0 & 0 & 1 \end{array}\right]}_{C_2}\right. x(t) + \underbrace{\left[\begin{array}{c} 1 \end{array}\right]}_{N_2} F_o(t)$$

The scalar variable A_f (in this case) has been chosen as $A_f = 1$. The new augmented system output in (51) is

$$\underbrace{\begin{bmatrix} y_1(t) \\ z_f(t) \end{bmatrix}}_{y_a} = \underbrace{\left[\begin{array}{ccccc} 1 & 0 & 0 & 0 & 0 \\ 0 & 1 & 0 & 0 & 0 \\ 0 & 0 & 1 & 0 & 0 \\ \hline 0 & 0 & 0 & 0 & 1 \end{array}\right]}_{C_a} \underbrace{\begin{bmatrix} x(t) \\ z_f(t) \end{bmatrix}}_{x_a} \tag{65}$$

As in Section IV-A, $L_{1_{aug}}$ was obtained using the code 'msfsyn' to place the closed-loop poles inside an LMI region [55], [56] to the left of a vertical line through -1. This yields $L_{1_{aug}} = [-2.9216\ \ -0.0000\ \ 0.9216]$ with

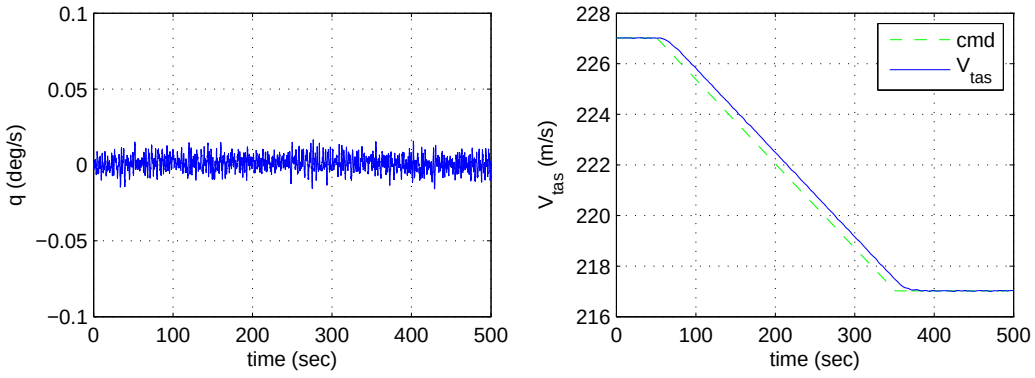

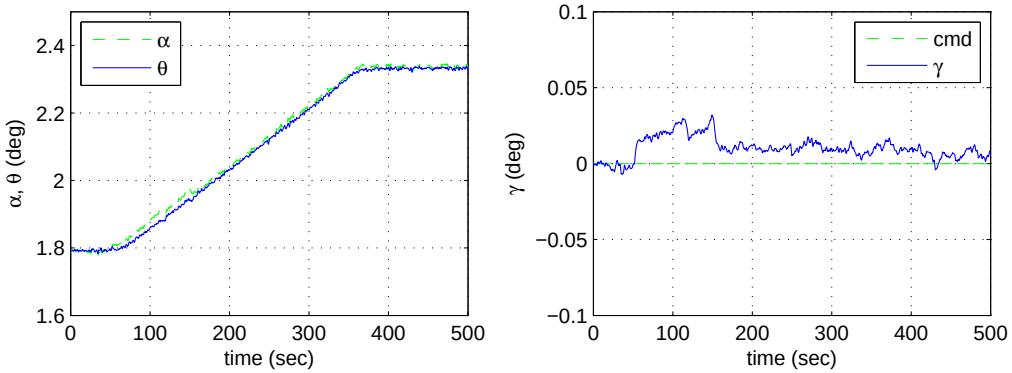

(a) States

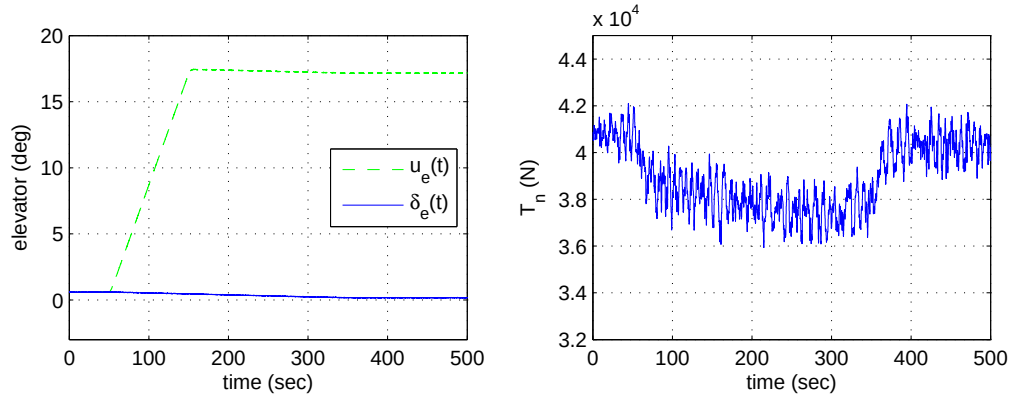

(b) Control surface deflections

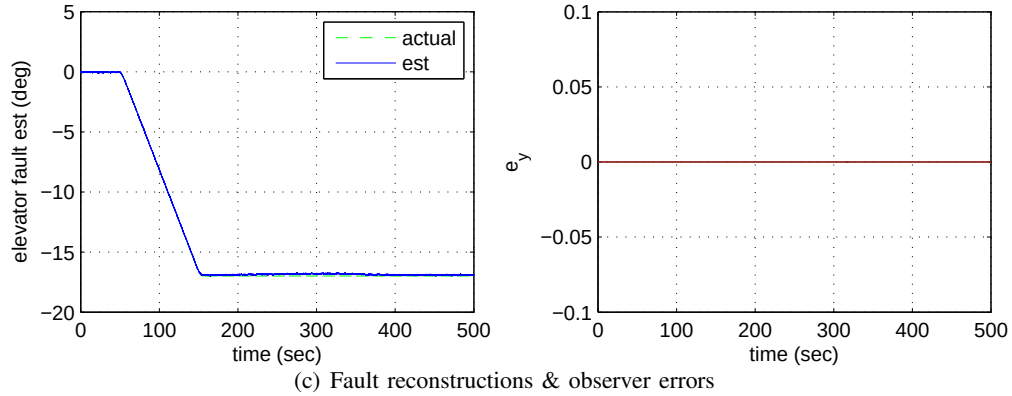

(c) Fault reconstructions & observer errors

Fig. 1. Nonlinear model simulation: elevator fault

$P_{1_{aug}} = 0.0582$. The stable design matrix $\tilde{A}^s_{22_{aug}}$ has been chosen as $\tilde{A}^s_{22_{aug}} = -0.9I_4$. The fixed gain $\tilde{G}_{n_{aug}}$ in (17) can be written in the original coordinates as $G_{n_{aug}} = T^{-1}_{o_{aug}} T^{-1}_{L_{aug}} \tilde{G}_{n_{aug}}$ and is given by

$$G_{n_{aug}} = \begin{bmatrix} 1.0000 & 0 & 0 & 0 \\ 0 & 1.0000 & 0 & 0 \\ 0 & 0 & 1.0000 & 0 \\ 2.9216 & 0.0000 & -0.9216 & 0 \\ 0 & 0 & 0 & 1.0000 \end{bmatrix}$$

As in Section IV-A, the gain $G_{l_{aug}}(\rho)$ in (22) has been split into varying and fixed components

$$\begin{aligned} G_{l_{aug}}(\rho) = T^{-1}_{o_{aug}} T^{-1}_{L_{aug}} \tilde{G}_l(\rho) &= T^{-1}_{o_{aug}} T^{-1}_{L_{aug}} \left(\begin{bmatrix} \tilde{A}_{12}(\rho) \\ \tilde{A}_{22}(\rho) \end{bmatrix} - \begin{bmatrix} 0 \\ \tilde{A}^s_{22_{aug}} \end{bmatrix} \right) \\ &= G_{la_{aug}}(\rho) - G_{lb_{aug}} \end{aligned}$$

where

$$G_{lb_{aug}} = \begin{bmatrix} -0.9000 & 0 & 0 & 0 \\ 0 & -0.9000 & 0 & 0 \\ 0 & 0 & -0.9000 & 0 \\ -2.6294 & -0.0000 & 0.8294 & 0 \\ 0 & 0 & 0 & -0.9000 \end{bmatrix}$$

and

$$G_{la_{aug}}(\rho) = G_{la_{aug0}} + \sum_{i=1}^{7} G_{la_{augi}} \rho_i$$

See the Appendix for details of the individual gains. The individual gains for the 'output injection signal' and the linear gains in (23), (25) and (26) are $k_{1_{aug}} = 2.1, k_{2_{aug}} = 0.9, k_{3_{aug}} = 2$ and $k_{4_{aug}} = 7.3289$.

A. Sensor Faults Reconstruction Results

The controller used in Section IV-B, was employed to effect a demand change in speed and altitude as shown in Figure 2(a). Note that the trim values are not considered in Figure 2. Also note that a change of altitude is outside the validity of the LPV model [53] used for the observer design. Here a change of altitude is used to show the capabilities of the sliding mode FDI scheme to handle model/plant mismatches.

It is assumed that the sensor fault only affects the fault monitoring unit (i.e. the faulty measurement only appears before the FDI observer) and the faulty sensor measurement (in this case θ) is not used by the controller in the feedback control loop. Note that as in Section IV-B, sensor noise was included in the simulation. The effect of noise can be seen in Figures 2(a) and 2(b).

Figure 2(a) displays the observer states $(q, V_{tas}, \alpha, \theta)$, the tracking of flight path angle (γ) and the change in altitude (h_e). Figure 2(a) also shows the corrupted measurement of θ (a slow drift from 50-400sec followed by a constant bias from 400sec onwards) and its filtered version z_f. Note that the effect of the filter is not visible (visibly both θ and z_f overlap). Figure 2(c) shows no visible errors between the actual measurements and the observer states as $\|e_y\|$ is close to zero. Figure 2(c) also shows good reconstruction of the faults by the proposed observer scheme.

VI. Conclusions

This paper has proposed a new LPV based sliding mode observer scheme for fault reconstruction. For actuator faults, the design involves factorizing the varying input distribution matrix associated with the fault channels into a fixed and varying part, creating a 'virtual' system. The observer gains, which are designed to ensure a stable reduced order sliding motion in the state estimation error space, are synthesized using LMI methods based on the virtual system. The virtual actuator fault reconstructions are based on the 'equivalent output error injection signals' of the observer, and are mapped back to create estimates of the actual faults by exploiting the factorization of the fault distribution matrix. For sensor faults, the observer design has involved re-formulating the problem into an

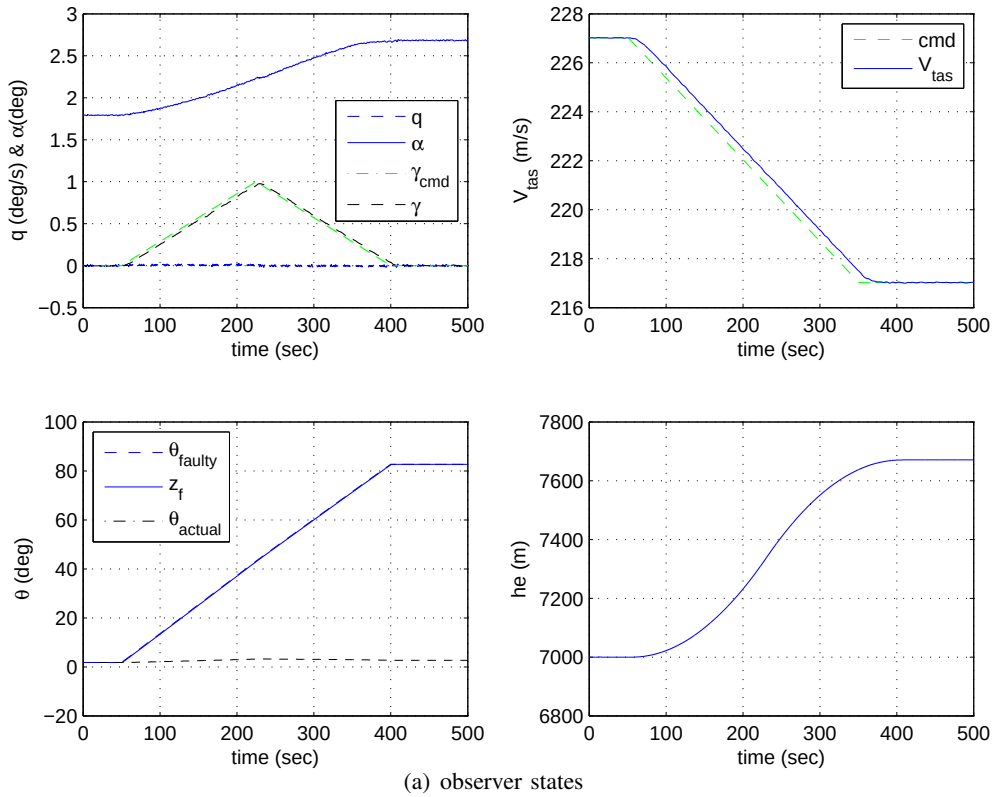

(a) observer states

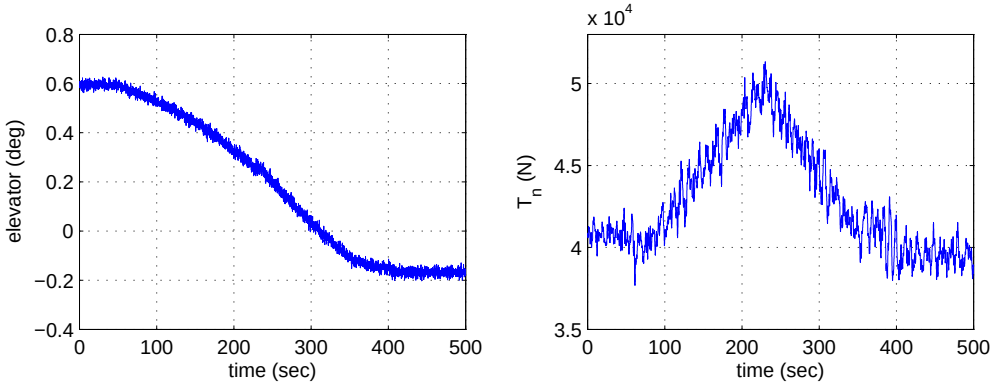

(b) control surface deflections

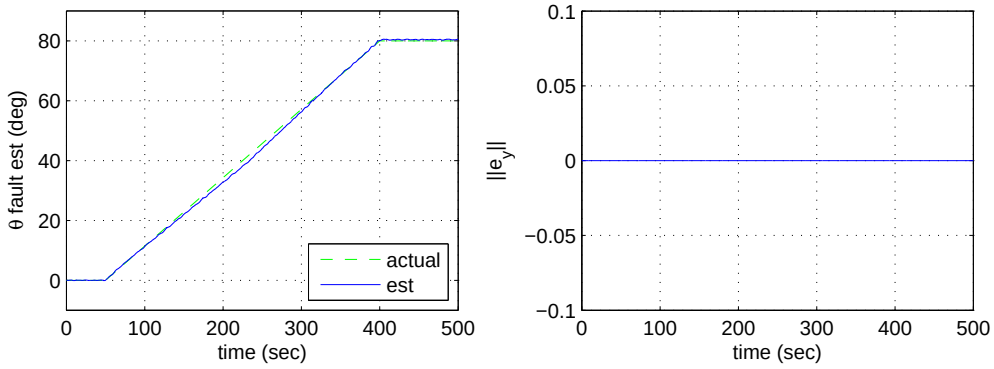

(c) fault reconstructions & observer errors

Fig. 2. Nonlinear model simulation: θ fault

actuator fault reconstruction framework. This allows the LPV observer synthesis approach for the actuator faults to be applied directly. The simulation results for both actuator and sensor faults, on the high fidelity nonlinear plant associated with the GARTEUR AG16 benchmark, show good reconstruction of the faults, demonstrating the efficacy of the proposed schemes.

APPENDIX

$$A(\rho) = \begin{bmatrix} 0 & 0 & 0 & a_{14}(\rho) \\ a_{21}(\rho) & a_{22}(\rho) & a_{23}(\rho) & 0 \\ 0 & a_{32}(\rho) & a_{33}(\rho) & a_{34}(\rho) \\ 0 & a_{42}(\rho) & a_{43}(\rho) & a_{44}(\rho) \end{bmatrix}$$

where

$$\begin{aligned}
a_{14}(\rho) &= 1 \\
a_{21}(\rho) &= -9.7851 \\
a_{22}(\rho) &= -0.0061 - 2.1091 \times 10^{-5}\rho_2 - 2.2374 \times 10^{-8}\rho_4 \\
a_{23}(\rho) &= 5.7733 - 84.5625\rho_1 - 0.0351\rho_2 - 0.7450\rho_3 - 7.7365 \times 10^{-5}\rho_4 - 0.0016\rho_5 \\
a_{32}(\rho) &= -5.2124 \times 10^{-4} - 6.2678 \times 10^{-7}\rho_2 + 1.1121 \times 10^{-11}\rho_4 \\
a_{33}(\rho) &= -0.5935 - 0.0026\rho_2 \\
a_{34}(\rho) &= 0.9914 \\
a_{42}(\rho) &= -4.9579 \times 10^{-4} - 3.8893 \times 10^{-6}\rho_2 - 7.6201 \times 10^{-9}\rho_4 + 1.9644 \times 10^{-12}\rho_6 \\
a_{43}(\rho) &= -1.9626 + 3.4170\rho_1 - 0.0173\rho_2 + 0.0301\rho_3 - 3.8081 \times 10^{-5}\rho_4 + 6.63 \times 10^{-5}\rho_6 \\
a_{44}(\rho) &= -0.4609 - 0.0020\rho_2
\end{aligned} \tag{66}$$

$$B(\rho) = \begin{bmatrix} 0 & 0 & 0 \\ 0 & 0 & b_{23}(\rho) \\ b_{31}(\rho) & 0 & b_{33}(\rho) \\ b_{41}(\rho) & b_{42}(\rho) & b_{43}(\rho) \end{bmatrix}$$

where

$$\begin{aligned}
b_{23}(\rho) &= 1.3323 \times 10^{-5} - 5.8133 \times 10^{-7}\rho_1 \\
b_{31}(\rho) &= -0.0358 - 1.1877 \times 10^{-5}\rho_2 + 1.5311 \times 10^{-6}\rho_4 + 3.9135 \times 10^{-9}\rho_6 \\
b_{33}(\rho) &= -3.6326 \times 10^{-9} - 5.8732 \times 10^{-8}\rho_1 + 1.6002 \times 10^{-11}\rho_2 + 2.5871 \times 10^{-10}\rho_3 \\
b_{41}(\rho) &= -1.7696 - 0.0089\rho_2 + 5.9851 \times 10^{-5}\rho_4 + 4.4285 \times 10^{-7}\rho_6 + 6.9127 \times 10^{-10}\rho_7 \\
b_{42}(\rho) &= -3.9993 - 0.0352\rho_2 - 7.7600 \times 10^{-5}\rho_4 \\
b_{43}(\rho) &= 1.5328 \times 10^{-7}
\end{aligned} \tag{67}$$

$$G_{la}(\rho) = \begin{bmatrix} 0 & 0 & g_{la13}(\rho) \\ g_{la21}(\rho) & g_{la22}(\rho) & 0 \\ g_{la31}(\rho) & g_{la32}(\rho) & g_{la33}(\rho) \\ g_{la41}(\rho) & g_{la42}(\rho) & g_{la43}(\rho) \end{bmatrix}$$

where

$$\begin{aligned}
g_{la13}(\rho) &= 1 \\
g_{la21}(\rho) &= 11.2232 - 2.1091 \times 10^{-5}\rho_2 - 2.2374 \times 10^{-8}\rho_4 \\
g_{la22}(\rho) &= 5.7733 - 84.5625\rho_1 - 0.0351\rho_2 - 0.7450\rho_3 - 7.7365 \times 10^{-5}\rho_4 - 0.0016\rho_5 \\
g_{la31}(\rho) &= -5.2124 \times 10^{-4} - 6.2678 \times 10^{-7}\rho_2 + 1.1121 \times 10^{-11}\rho_4 \\
g_{la32}(\rho) &= -0.5935 - 0.0026\rho_2 \\
g_{la33}(\rho) &= 0.9914 \\
g_{la41}(\rho) &= -4.9579 \times 10^{-4} - 3.8893 \times 10^{-6}\rho_2 - 7.6201 \times 10^{-9}\rho_4 + 1.9644 \times 10^{-12}\rho_6 \\
g_{la42}(\rho) &= -1.9626 + 3.4170\rho_1 - 0.0173\rho_2 + 0.0301\rho_3 - 3.8081 \times 10^{-5}\rho_4 + 6.63 \times 10^{-5}\rho_6 \\
g_{la43}(\rho) &= -0.4609 - 0.0020\rho_2
\end{aligned} \tag{68}$$

$$G_{la_{aug}}(\rho) = \begin{bmatrix} g_{la_{aug}11}(\rho) & g_{la_{aug}12}(\rho) & g_{la_{aug}13}(\rho) & 0 \\ g_{la_{aug}21}(\rho) & g_{la_{aug}22}(\rho) & g_{la_{aug}23}(\rho) & 0 \\ g_{la_{aug}31}(\rho) & 0 & g_{la_{aug}33}(\rho) & 0 \\ 0 & g_{la_{aug}42}(\rho) & 0 & 0 \\ g_{la_{aug}51}(\rho) & g_{la_{aug}52}(\rho) & g_{la_{aug}53}(\rho) & g_{la_{aug}54}(\rho) \end{bmatrix}$$

where

$$\begin{aligned}
g_{la_{aug}11}(\rho) &= -0.5935 - 0.0026\rho_2 \\
g_{la_{aug}12}(\rho) &= 0.9914 \\
g_{la_{aug}13}(\rho) &= -5.2124 \times 10^{-4} - 6.2678 \times 10^{-7}\rho_2 + 1.1121 \times 10^{-11}\rho_4 \\
g_{la_{aug}21}(\rho) &= -1.9626 + 3.4170\rho_1 - 0.0173\rho_2 + 0.0301\rho_3 - 3.8081 \times 10^{-5}\rho_4 + 6.63 \times 10^{-5}\rho_6 \\
g_{la_{aug}22}(\rho) &= -0.4609 - 0.0020\rho_2 \\
g_{la_{aug}23}(\rho) &= -4.9579 \times 10^{-4} - 3.8893 \times 10^{-6}\rho_2 - 7.6201 \times 10^{-9}\rho_4 + 1.9644 \times 10^{-12}\rho_6 \\
g_{la_{aug}31}(\rho) &= -22.8150 - 84.5625\rho_1 - 0.0351\rho_2 - 0.7450\rho_3 - 7.7365 \times 10^{-5}\rho_4 - 0.0016\rho_5 \\
g_{la_{aug}33}(\rho) &= 1.4939 - 2.1091 \times 10^{-5}\rho_2 - 2.2374 \times 10^{-8}\rho_4 \\
g_{la_{aug}42}(\rho) &= 1 \\
g_{la_{aug}51}(\rho) &= 2.9216 \\
g_{la_{aug}52}(\rho) &= 7.9363 \times 10^{-3} \\
g_{la_{aug}53}(\rho) &= -0.9216 \\
g_{la_{aug}54}(\rho) &= -1
\end{aligned} \tag{69}$$

REFERENCES

[1] R. Patton, Robustness in model-based fault diagnosis: the 1997 situation, IFAC Annual Reviews 21 (1997) 101–121.

[2] Y. Zhang, J. Jiang, Bibliographical review on reconfigurable fault tolerant control systems, in: Proceedings of the IFAC Symposium SAFEPROCESS '03, Washington, 2003, pp. 265–276.

[3] E. Alcorta-Garcia, A. Zolghadri, P. Goupil, A novel non-linear observer-based approach to oscillatory failure detection, in: European Control Conference, 2009, pp. 1901–1906.

[4] F. Amato, M. Mattei, R. Iervolino, G. Paviglianiti, A nonlinear UIO scheme for the FDI on a small commercial aircraft, in: IEEE International Conference on Control Applications, 2002, pp. 235–240.

[5] P. Castaldi, W. Geri, M. Bonfé, S. Simani, M. Benini, Design of residual generators and adaptive filters for the FDI of aircraft model sensors, Control Engineering Practice 18 (5) (2010) 449–459.

[6] M. O. Abdalla, E. G. Nobrega, K. M. Grigoriadis, Fault detection and isolation filter design for linear parameter varying systems, in: Proceedings of the American Control Conference, 2001, pp. 3890 – 3895.

[7] A. Marcos, S. Ganguli, G. J. Balas, An application of H_∞ fault detection and isolation to a transport aircraft, Control Engineering Practice 13 (1) (2005) 105–119.

[8] J. Chen, R. J. Patton, Robust Model-Based Fault Diagnosis for Dynamic Systems, Kluwer Academic Publishers, 1999.

[9] N. E. Wu, Y. Zhang, K. Zhou, Control effectiveness estimation using an adaptive Kalman estimator, in: Proceedings of the 1998 IEEE International Symposium on Intelligent Control (ISIC) held jointly with IEEE International Symposium on Computational Intelligence in Robotics and Automation (CIRA) Intelligent Systems and Semiotics (ISAS), 1998, pp. 181–6.

[10] G. J. Balas, Linear, parameter–varying control and its application to a turbofan engine, International Journal of Robust and Nonlinear Control 12 (2002) 763–796.

[11] J. Bokor, G. Balas, Detection filter design for LPV systems - a geometric approach, Automatica 40 (2004) 511–518.
[12] R. Hallouzi, V. Verdult, R. Babuska, M. Verhaegen, Fault detection and identification of actuator faults using linear parameter varying models, in: Preprints of the IFAC World Congress, 2005.
[13] J. Bokor, Z. Szabo, G. Stikkel, Failure detection for quasi LPV systems, in: IEEE Conference on Decision and Control, 2002.
[14] S. Grenaille, D. Henry, A. Zolghadri, A method for designing fault diagnosis filters for LPV polytopic systems, Journal of Control Science and Engineering 2008 (doi:10.1155/2008/231697) (2008) 1–11.
[15] S. Armeni, A. Casavola, E. Mosca, Robust fault detection and isolation for LPV systems under a sensitivity constraint, International Journal Of Adaptive Control And Signal Processing 23 (2009) 55–72.
[16] I. Szaszi, A. Marcos, G. J. Balas, J. Bokor, Linear parameter-varying detection filter design for a Boeing 747-100/200 aircraft, Journal of Guidance, Control, and Dynamics 28 (3) (2005) 461–470.
[17] G. Becker, A. Packard, D. Philbrick, G. Balas, Control of parametrically-dependent linear systems a single quadratic lyapunov approach, in: American Control Conference, 1993, pp. 2795–99.
[18] P. Apkarian, P. Gahinets, G. Becker, Self-scheduled $\mathcal{H}_\infty$ control of linear parameter-varying systems: a design example, Automatica 31 (9) (1995) 1251–1261.
[19] F. Wu, Control of linear parameter varying systems, Ph.D. thesis, University of California at Berkeley (1995).
[20] G. Papageorgiou, Robust control systems design h-infinity loop shaping and aerospace applications, Ph.D. thesis, University of Cambridge (1998).
[21] S. Ganguli, A. Marcos, G. J. Balas, Reconfigurable LPV control design for Boeing 747-100/200 longitudinal axis, in: American Control Conference, 2002, pp. 3612–3617.
[22] A. Casavola, D. Famularo, G. Franz, M. Sorbara, A fault-detection, filter-design method for linear parameter-varying systems, Proceedings of the Institution of Mechanical Engineers, Part I: Journal of Systems and Control Engineering 221 (6) (2007) 865–874.
[23] M. Sato, Filter design for LPV systems using quadratically parameter-dependent lyapunov functions, Automatica 42 (11) (2006) 2017–2023.
[24] D. Henry, A. Falcoz, A. Zolghadri, Structured h_∞/h_- LPV filters for fault diagnosis: Some new results, in: Proceedings of the IFAC Symposium SAFEPROCESS '09, Barcelona, 2009, pp. 420–425.
[25] F. Hermans, M. Zarrop, Sliding mode observers for robust sensor monitoring, in: Proceedings of the 13th IFAC World Congress, 1996, pp. 211–216.
[26] H. Yang, M. Saif, Fault detection in a class of nonlinear systems via adaptive sliding observer, in: Proceedings of the IEEE International Conference on Systems, Man and Cybernetics, 1995, pp. 2199–2204.
[27] Y. M. Zhang, J. Jiang, Active fault-tolerant control system against partial actuator failures, IEE Proceedings: Control Theory & Applications 149 (2002) 95–104.
[28] Y. W. Kim, G. Rizzoni, V. Utkin, Developing a fault tolerant power train system by integrating the design of control and diagnostics, International Journal of Robust and Nonlinear Control 11 (2001) 1095–1114.
[29] C. Edwards, C. P. Tan, Sensor fault tolerant control using sliding mode observers, Control Engineering Practice 16 (2006) 897–908.
[30] H. Alwi, C. Edwards, Fault detection and fault-tolerant control of a civil aircraft using a sliding-mode-based scheme, IEEE Transactions on Control Systems Technology 16 (3) (2008) 499–510.
[31] C. Edwards, S. Spurgeon, R. Patton, Sliding mode observers for fault detection, Automatica 36 (2000) 541–553.
[32] C. P. Tan, C. Edwards, An LMI approach for designing sliding mode observers, International Journal of Control 74 (2001) 1559–1568.
[33] C. P. Tan, C. Edwards, Sliding mode observers for robust detection and reconstruction of actuator and sensor faults, International Journal of Robust and Nonlinear Control 13 (2003) 443–463.
[34] X. G. Yan, C. Edwards, Nonlinear robust fault reconstruction and estimation using a sliding mode observer, Automatica 43 (9) (2007) 1605–1614.
[35] S. Sivrioglu, K. Nonami, Sliding mode control with time-varying hyperplane for AMB systems, IEEE/ASME Transactions On Mechatronics 3 (1) (1998) 51–59.
[36] K. Nonami, S. Sivrioglu, Sliding mode control with gain scheduled hyperplane for LPV plant, in: K. D. Young, U. Özgüner (Eds.), Variable structure systems, sliding mode and nonlinear control, Vol. 247 of Lecture Notes in Control and Information Sciences, Springer Berlin / Heidelberg, 1999, pp. 263–279.
[37] L. Fridman, Y. Shtessel, C. Edwards, X. Yan, Higher-order sliding-mode observer for state estimation and input reconstruction in nonlinear systems, International Journal of Robust and Nonlinear Control 18 (4-5) (2008) 399412.
[38] C. Hanke, D. Nordwall, The simulation of a jumbo jet transport aircraft. Volume II: Modelling data, Tech. Rep. CR-114494/D6-30643-VOL2, NASA and The Boeing Company (1970).
[39] C. Hanke, The simulation of a large jet transport aircraft. Volume I: Mathematical model, Tech. Rep. CR-1756, NASA and the Boeing company (1971).
[40] A. Marcos, G. J. Balas, A Boeing 747–100/200 aircraft fault tolerant and diagnostic benchmark, Tech. Rep. AEM–UoM–2003–1, Department of Aerospace and Engineering Mechanics, University of Minnesota (2003).
[41] C. Edwards, T. Lombaerts, H. S. (Eds.), Fault Tolerant Flight Control: A Benchmark Challenge, Vol. 399, Springer-Verlag: Lecture Notes in Control and Information Sciences, 2010.
[42] C. Edwards, S. K. Spurgeon, Sliding Mode Control: Theory and Applications, Taylor & Francis, 1998.
[43] J. A. Moreno, M. Osorio, A Lyapunov approach to second-order sliding mode controllers and observers, in: 47th IEEE Conference on Decision and Control, 2008, pp. 2856–2861.
[44] P. Goupil, AIRBUS state of the art and practices on FDI and FTC, in: Proceedings of the IFAC Symposium SAFEPROCESS '09, Barcelona, 2009, pp. 564–572.
[45] C. A. A. M. van der Linden, DASMAT: Delft University aircraft simulation model and analysis tool, Tech. Rep. LR–781, Technical University of Delft, the Netherlands (1996).

[46] M. H. Smaili, Flightlab 747: Benchmark for advance flight control engineering, Tech. rep., Technical University Delft, the Netherlands (1999).
[47] Anon, El al flight 1862, aircraft accident report 92-11, Tech. rep., Netherlands Aviation Safety Board, Hoofddorp (1994).
[48] M. H. Smaili, J. A. Mulder, Flight data reconstruction and simulation of the 1992 Amsterdam Bijlmermeer airplane accident, in: AIAA Modeling and Simulation Technologies Conference, 2000.
[49] A. Hennig, G. J. Balas, MPC supervisory flight controller: A case study to flight EL AL 1862, in: AIAA Guidance, Navigation and Control Conference and Exhibit, 2008.
[50] A. Marcos, G. J. Balas, A robust integrated controller/diagnosis aircraft application, International Journal of Robust and Nonlinear Control 15 (12) (2005) 531–551.
[51] K. Zhou, P. K. Rachinayani, N. Liu, Z. Ren, J. Aravna, Fault diagnosis and reconfigurable control for flight control systems with actuator failures, in: 43rd IEEE Conference on Decision and Control, Bahamas, 2004.
[52] H. Smaili, J. Breeman, T. Lombaerts, D. Joosten, Recover: A benchmark for integrated fault tolerant flight control evaluation, in: C. Edwards, T. Lombaerts, H. Smaili (Eds.), Fault Tolerant Flight Control, Vol. 399 of Lecture Notes in Control and Information Sciences, Springer Berlin / Heidelberg, 2010, pp. 171–221.
[53] T. H. Khong, J. Shin, Robustness analysis of integrated LPV-FDI filters and LTI-FTC system for a transport aircraft, in: AIAA Guidance, Navigation and Control Conference and Exhibit, no. AIAA 2007-6771, 2007.
[54] A. Marcos, G. J. Balas, Development of linear-parameter-varying models for aircraft, AIAA Journal of Guidance, Control and Dynamics 27 (2) (2004) 218–228.
[55] P. Gahinet, A. Nemirovski, A. Laub, M. Chilali, LMI Control Toolbox, User Guide, MathWorks, Inc., 1995.
[56] M. Chilali, P. Gahinet, $\mathcal{H}_\infty$ design with pole placement constraints: an LMI approach, IEEE Transactions on Automatic Control AC-41 (1996) 358–367.
[57] T. Floquet, C. Edwards, S. K. Spurgeon, On sliding mode observers for systems with unknown inputs, International Journal of Adaptive Control and Signal Processing 21 (2007) 638–656.